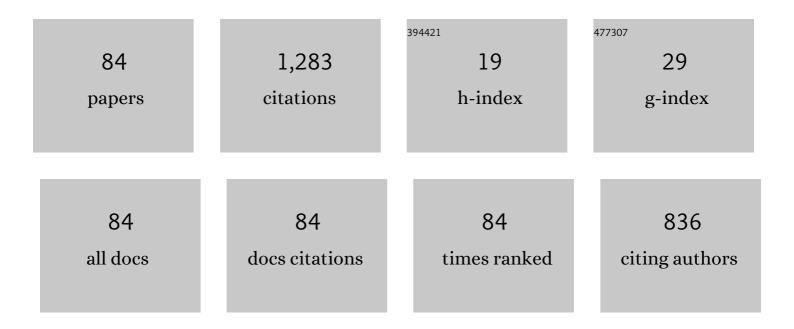
List of Publications by Year in descending order

Source: https://exaly.com/author-pdf/2858437/publications.pdf Version: 2024-02-01



#	Article	IF	CITATIONS
1	Phase-Selective Distribution of Eu ²⁺ and Eu ³⁺ in Oxide and Fluoride Crystals in Glass-Ceramics for Warm White-Light-Emitting Diodes. ACS Applied Electronic Materials, 2019, 1, 961-971.	4.3	61
2	Crystallization behavior of sodium iron phosphate glass Na2â^'Fe1+0.5P2O7 for sodium ion batteries. Journal of Non-Crystalline Solids, 2014, 404, 26-31.	3.1	53
3	Electrical conductivity of Na2O–Nb2O5–P2O5 glass and fabrication of glass–ceramic composites with NASICON type Na3Zr2Si2PO12. Solid State Ionics, 2015, 269, 19-23.	2.7	53
4	Optical and magneto-optical properties of Bi substituted yttrium iron garnets prepared by metal organic decomposition. Optical Materials Express, 2016, 6, 1986.	3.0	43
5	Morphology of CaF2 nanocrystals and elastic properties in transparent oxyfluoride crystallized glasses. Optical Materials, 2011, 33, 1350-1356.	3.6	41
6	High quantum yield and low concentration quenching of Eu3+ emission in oxyfluoride glass with high BaF2 and Al2O3 contents. Optical Materials, 2014, 36, 1384-1389.	3.6	41
7	Near-infrared engineering for broad-band wavelength-tunable in biological window of NIR-â; and -â¢: A solid solution phosphor of Sr1-xCaxTiO3:Ni2+. Journal of Luminescence, 2021, 238, 118235.	3.1	38
8	Radio-photoluminescence in Sm-doped BaF2-Al2O3-B2O3 glass-ceramics. Radiation Measurements, 2017, 106, 73-78.	1.4	37
9	Massive red shift of Ce ³⁺ in Y ₃ Al ₅ O ₁₂ incorporating super-high content of Ce. RSC Advances, 2020, 10, 12535-12546.	3.6	32
10	New oxyfluoride glass with high fluorine content and laser patterning of nonlinear optical BaAlBO3F2 single crystal line. Journal of Applied Physics, 2012, 112, .	2.5	31
11	Scintillation properties of Ce-doped SrF2-Al2O3-B2O3 glasses. Journal of Non-Crystalline Solids, 2019, 508, 46-50.	3.1	30
12	Glass structure and NIR emission of Er3+ at 1.5 μm in oxyfluoride BaF2–Al2O3–B2O3 glasses. Optical Materials, 2015, 50, 238-243.	3.6	29
13	Morphology and photoluminescence properties of Er3+-doped CaF2 nanocrystals patterned by laser irradiation in oxyfluoride glasses. Journal of Fluorine Chemistry, 2013, 145, 81-87.	1.7	28
14	Elastic properties and Vickers hardness of optically transparent glass–ceramics with fresnoite Ba2TiSi2O8 nanocrystals. Materials Research Bulletin, 2011, 46, 922-928.	5.2	27
15	Aluminum for Near Infrared Plasmonics: Amplified Up onversion Photoluminescence from Core–Shell Nanoparticles on Periodic Lattices. Advanced Optical Materials, 2021, 9, .	7.3	27
16	Electronic polarizability and interaction parameter of gadolinium tungsten borate glasses with high WO3 content. Journal of Solid State Chemistry, 2014, 220, 191-197.	2.9	25
17	Morphology and dispersion state of Ba2TiSi2O8 nanocrystals in transparent glass-ceramics and their nanoindentation behavior. Journal of Non-Crystalline Solids, 2012, 358, 1863-1869.	3.1	22
18	Luminescence of Ce 3+ in aluminophosphate glasses prepared in air. Journal of Luminescence, 2018, 195, 413-419.	3.1	21

#	Article	IF	CITATIONS
19	Morphology and orientation of β-BaB2O4 crystals patterned by laser in the inside of samarium barium borium borate glass. Journal of Solid State Chemistry, 2015, 221, 145-151.	2.9	20
20	Preparation and scintillation properties of the Eu3+-activated SrO–Al2O3–TeO2 glasses. Materials Research Bulletin, 2022, 145, 111547.	5.2	20
21	Structural study of WO3-La2O3-B2O3-Nb2O5 glasses. Journal of Non-Crystalline Solids, 2020, 543, 120132.	3.1	20
22	Fluorine deficient layer at the surface of transparent glass-ceramics with CaF2 nanocrystals. Journal of Physics and Chemistry of Solids, 2012, 73, 683-687.	4.0	19
23	Radio-photoluminescence observed in Eu-doped BABF glass-ceramics. Ceramics International, 2019, 45, 9376-9380.	4.8	19
24	X-ray induced luminescence properties of Ce-doped BaF2-Al2O3-B2O3 glasses. Optical Materials, 2019, 90, 64-69.	3.6	18
25	Synthesis and morphology of Ba1â^'RE2/3Nb2O6 nanocrystals with tungsten bronze structure in RE2O3–BaO–Nb2O5–B2O3 glasses (RE: Sm, Eu, Gd, Dy, Er). Journal of Solid State Chemistry, 2012, 196, 384-390.	2.9	17
26	Synthesis and photocatalytic properties of α-ZnWO4 nanocrystals in tungsten zinc borate glasses. Journal of Asian Ceramic Societies, 2014, 2, 253-257.	2.3	17
27	Structure of MoO3–WO3–La2O3–B2O3 glasses and crystallization of LaMo1â^'xWxBO6 solid solutions. Journal of Non-Crystalline Solids, 2015, 429, 171-177.	3.1	17
28	Tb3+-doped BaF2-Al2O3-B2O3 glass and glass-ceramic for radiation measurements. Journal of Non-Crystalline Solids, 2018, 501, 111-115.	3.1	17
29	Scintillation and TSL properties of Nd-doped TeO2–Al2O3-WO3 glasses. Solid State Sciences, 2020, 100, 106111.	3.2	17
30	Scintillation properties of organic–inorganic layered perovskite nanocrystals in glass. Journal of Applied Physics, 2020, 127, .	2.5	16
31	Photoluminescence and scintillation properties of Al(PO3)3–CeCl3–CsCl–CsPO3 glass scintillators. Journal of Materials Science: Materials in Electronics, 2020, 31, 4488-4493.	2.2	16
32	TEM analysis for crystal structure of metastable BiBO3 (II) phase formed in glass by laser-induced crystallization. Journal of the European Ceramic Society, 2015, 35, 2541-2546.	5.7	15
33	Long afterglow in hexagonal SrAl2O4:Eu2+, Dy3+ synthesized by crystallization of glass and solidification of supercooled melts. Journal of Luminescence, 2016, 177, 286-289.	3.1	15
34	Scintillator and dosimeter properties of Ce3+ doped CaF2AlF3AlPO4 glasses. Optical Materials, 2019, 94, 86-91.	3.6	15
35	Synthesis of new transparent borate-based BaF2 nanocrystallized glass by formation of nucleation sites induced by rare earth ions. Journal of the European Ceramic Society, 2019, 39, 1735-1739.	5.7	15
36	Coexistence of nano-scale phase separation and micro-scale surface crystallization in Gd2O3–WO3–B2O3 glasses. Journal of Non-Crystalline Solids, 2013, 381, 17-22.	3.1	14

#	Article	IF	CITATIONS
37	Scintillation and VUV-excited photoluminescence of europium-doped BaF2–Al2O3–B2O3 glasses. Journal of Materials Science: Materials in Electronics, 2018, 29, 11824-11829.	2.2	14
38	Dosimetric, luminescence and scintillation properties of Ce-doped CaF2-Al2O3-B2O3 glasses. Journal of Non-Crystalline Solids, 2019, 509, 60-64.	3.1	14
39	Up-conversion Luminescence Enhanced by the Plasmonic Lattice Resonating at the Transparent Window of Water. ACS Applied Energy Materials, 2021, 4, 2999-3007.	5.1	14
40	Toughening silica glass by imparting ductility using a small amount of silver nanoparticles. Materials Science & Engineering A: Structural Materials: Properties, Microstructure and Processing, 2021, 817, 141372.	5.6	14
41	Electrochemical performance as cathode of lithium iron silicate, borate and phosphate glasses with different Fe2+ fractions. Journal of Non-Crystalline Solids, 2016, 436, 51-57.	3.1	13
42	Nano-crystallization and highly oriented crystal line patterning of Sm3+-doped Bi2GeO5 and Bi4Ge3O12 in bismuth germanate-based glasses. Journal of Non-Crystalline Solids, 2017, 459, 116-122.	3.1	12
43	Photoluminescence and scintillation properties of Eu-doped TeO2-Al2O3-BaO glasses. Journal of Materials Science: Materials in Electronics, 2019, 30, 11468-11474.	2.2	12
44	Optical and radiation response characteristics of Eu2O3-doped K2O–Bi2O3–Ga2O3 glasses. Ceramics International, 2021, 47, 11596-11601.	4.8	12
45	In Situ Growth Mechanism of CsPbX ₃ (X = Cl, Br, and I) Quantum Dots in an Amorphous Oxide Matrix. Chemistry of Materials, 2022, 34, 1599-1610.	6.7	12
46	Self-organized homo-epitaxial growth in nonlinear optical BaAlBO3F2 crystal crossing lines patterned by laser in glass. Optical Materials, 2015, 49, 182-189.	3.6	11
47	Characterizations of Pr-doped Yb3Al5O12 single crystals for scintillator applications. Solid State Sciences, 2018, 78, 1-6.	3.2	11
48	Preparation of calcium phosphate nanoparticles hybridized with europium(III) complex for novel luminescent organic-inorganic systems. Journal of Physics and Chemistry of Solids, 2018, 122, 218-226.	4.0	11
49	Optical, scintillation and thermoluminescent properties of Eu2O3-doped K2O–La2O3–Ga2O3 glasses. Radiation Physics and Chemistry, 2022, 190, 109785.	2.8	11
50	Scintillation properties of Dy-doped TeO ₂ –Al ₂ O ₃ –BaO glasses. Journal of the Ceramic Society of Japan, 2020, 128, 1024-1029.	1.1	11
51	Laser Patterning of Non-Linear Optical Bi2ZnB2O7 Crystal Lines in Glass. Frontiers in Materials, 2015, 2,	2.4	9
52	Effect of Mg ²⁺ and fluorine on the network and highly efficient photoluminescence of Eu ³⁺ ion in MgF ₂ –BaO–B ₂ O ₃ glasses. Journal of the American Ceramic Society, 2019, 102, 2531-2541.	3.8	9
53	Photo-, radio- and thermo- luminescence properties of Eu-doped BaSi2O5 glass-ceramics. Optik, 2019, 185, 812-818.	2.9	9
54	Rapid Synthesis of Quantum-Sized Organic–Inorganic Perovskite Nanocrystals in Glass. Scientific Reports, 2020, 10, 1237.	3.3	9

#	Article	IF	CITATIONS
55	Radiation Response Characteristics of Pr3+-activated SrO–Al2O3–TeO2 Glasses. Sensors and Materials, 2022, 34, 707.	0.5	9
56	Unique thermal conductivity, Young's modulus and local structure of 72SnO–28P ₂ O ₅ glass. Journal of the Ceramic Society of Japan, 2016, 124, 606-612.	1.1	8
57	Radiation response properties of Eu3+-doped K2O–Ta2O5–Ga2O3 glasses. Ceramics International, 2022, 48, 9353-9361.	4.8	8
58	Scintillation characteristics of Eu2O3-doped WO3–Al2O3–TeO2 glasses. Journal of Luminescence, 2022, 249, 119003.	3.1	8
59	Dielectric properties of glass-ceramics with Ba1â^'xY2x/3Nb2O6 nanocrystals and laser patterning of highly oriented crystal lines. Journal of Non-Crystalline Solids, 2016, 452, 74-81.	3.1	7
60	Improvement in microstructure and thermo-mechanical properties of MgO-based dry vibratable material by addition of Fe. Materials Chemistry and Physics, 2020, 253, 123368.	4.0	7
61	Impact of crystallization method on the strain, defect formation, and thermoluminescence of YAG:Ce crystals. Journal of Alloys and Compounds, 2020, 849, 156600.	5.5	7
62	Formation of highly dispersed tin nanoparticles in amorphous silicates for sodium ion battery anode. Journal of Physics and Chemistry of Solids, 2022, 161, 110377.	4.0	7
63	Effect of AlN addition on spatial uniform distribution of Er ³⁺ -doped CaF ₂ nanocrystals in oxyfluoride glass-ceramics. Journal of the Ceramic Society of Japan, 2013, 121, 457-459.	1.1	6
64	Highly efficient red-emitting BaMgBO3F:Eu3+,R+(R: Li, Na, K, Rb) phosphor for near-UV excitation synthesized via glass precursor solid-state reaction. Japanese Journal of Applied Physics, 2017, 56, 092601.	1.5	6
65	Photoluminescence and structural similarity of crystals with oxide–fluoride stacking structure and oxyfluoride glass. Journal of the Ceramic Society of Japan, 2020, 128, 1030-1037.	1.1	6
66	Fracture toughness enhancement via subâ€micro silverâ€precipitation in silica glass fabricated by spark plasma sintering. Journal of the American Ceramic Society, 2022, 105, 1980-1991.	3.8	6
67	Interfacial heterogeneous precipitation of Ag nanoparticles in soda-lime silicate glass for improved toughness and conductivity. Ceramics International, 2021, 47, 24466-24475.	4.8	5
68	Simultaneous surface and bulk crystallization of Bi _{1.5} ZnNb _{1.5} O ₇ â€ŧype pyrochlores and related crystals in glasses. International Journal of Applied Glass Science, 2018, 9, 296-304.	2.0	4
69	Control of self-powdering phenomenon in ferroelastic β′-Gd2(MoO4)3 crystallization in boro-tellurite glasses. Journal of Non-Crystalline Solids, 2018, 501, 85-92.	3.1	4
70	Design of crystallization of oxyfluoride glasses based on the local structure of fluorine. Journal of the Ceramic Society of Japan, 2018, 126, 684-692.	1.1	4
71	Structural origin of high-density Gd2O3–MoO3–B2O3 glass and low-density β′-Gd2(MoO4)3 crystal: a study conducted using high-energy x-ray diffraction and EXAFS at high temperatures. Journal of Physics Condensed Matter, 2020, 32, 055705.	1.8	4
72	Synthesis of Luminescent Eu(III)-Doped Octacalcium Phosphate Particles Hybridized with Succinate Ions and Their Reactive Behavior in Simulated Body Fluid. Crystal Growth and Design, 2021, 21, 2005-2018.	3.0	4

#	Article	IF	CITATIONS
73	Microstructure and improved fracture toughness of borosilicate glass reinforced by 1 vol% Ag nanoparticles. Ceramics International, 2022, 48, 30900-30904.	4.8	4
74	A Simple Incorporation Route of Tris(8-hydroxyquinoline)aluminum(III) into Transparent Mesoporous Silica Films and Their Photofunctions. Hindawi Journal of Chemistry, 2017, 2017, 1-10.	1.6	3
75	Scintillation characteristics of Nd ³⁺ -doped BaO–Al ₂ O ₃ –TeO ₂ glasses. Japanese Journal of Applied Physics, 2022, 61, SB1034.	1.5	3
76	Ultrafast Nanocrystallization of BaF ₂ in Oxyfluoride Glasses with Crystal-like Nanostructures: Implications for Upconversion Fiber Devices. ACS Applied Nano Materials, 2022, 5, 4281-4292.	5.0	3
77	Plasmonic Enhancement of Upconversion Photoluminescence from CaF ₂ : Er ³⁺ , Yb ³⁺ Nanoparticles on TiN Nanoantennas. Funtai Oyobi Fummatsu Yakin/Journal of the Japan Society of Powder and Powder Metallurgy, 2020, 67, 140-145.	0.2	2
78	Self‣training Nanocrystals Strategy: Temperature and Pressure Coâ€Induced Phase Transitions of CsPbBr ₃ in Amorphous Matrices. Advanced Optical Materials, 0, , 2200818.	7.3	2
79	Nanoindentation Analysis of Elastic/Mechanical Behaviour of Surface of Transparent Glass Ceramics with Fresnoite Ba2TiSi2O8Nanocrystals. IOP Conference Series: Materials Science and Engineering, 2011, 21, 012020.	0.6	1
80	Enhancement of photoluminescence of glass phosphor by nanoimprint of moth-eye structure. Journal of the Ceramic Society of Japan, 2017, 125, 766-769.	1.1	1
81	Utility of Tissue Classification in Invasive Ductal Carcinoma using Dynamic Magnetic Resonance Imaging of the Mammary Gland. Journal of Clinical Imaging Science, 2021, 11, 4.	1.1	0
82	Enhanced growth of Y3al5O12:Ce3+ nanocrystals in mesoporous SiO2 utilizing vacuum-assisted impregnation. Processing and Application of Ceramics, 2020, 14, 141-145.	0.8	0
83	Development of Photo-functional Glasses with Nanostructure Induced though Bond Selectivity in Oxyfluoride. Funtai Oyobi Fummatsu Yakin/Journal of the Japan Society of Powder and Powder Metallurgy, 2022, 69, 68-72.	0.2	0
84	Thermal conductivity and mechanical properties of soda-lime glass with interfacially connected Au layer fabricated via sputtering and spark plasma sintering. Journal of Asian Ceramic Societies, 0, , 1-6.	2.3	0